ANL-ART-255
ANL-METL-40

Flow Sensor Test Article (F-STAr) – Design and Fabrication Status Report

Nuclear Science and Engineering Division

About Argonne National Laboratory

Argonne is a U.S. Department of Energy laboratory managed by UChicago Argonne, LLC under contract DE-AC02-06CH11357. The Laboratory's main facility is outside Chicago, at 9700 South Cass Avenue, Argonne, Illinois 60439. For information about Argonne and its pioneering science and technology programs, see http://www.anl.gov.

Disclaimer

ANL-ART-255
ANL-METL-40

Flow Sensor Test Article (F-STAr) – Design and Fabrication Status Report

J. Rein, M. Weathered, E. Kent, D. Kultgen, C. Grandy

Nuclear Science and Engineering Division
Argonne National Laboratory

August 2022

Contents

List of Figures

List of Tables

1 Executive Summary

The Flow Sensor Test Article (F-STAr) is a test article currently under construction for the Mechanisms Engineering Test Loop (METL). F-STAr was designed to provide high sodium flowrate capabilities for sensor calibration, component testing, and fluid studies. Figure 1 shows two solid model views of the new test article. F-STAr includes a high-capacity pump that can provide a nominal flowrate of 120 GPM; a test section support structure that can accommodate a wide array of sub-test articles and their instrumentation; and finally, a heating and cooling system to aid in controlling the testing environment.

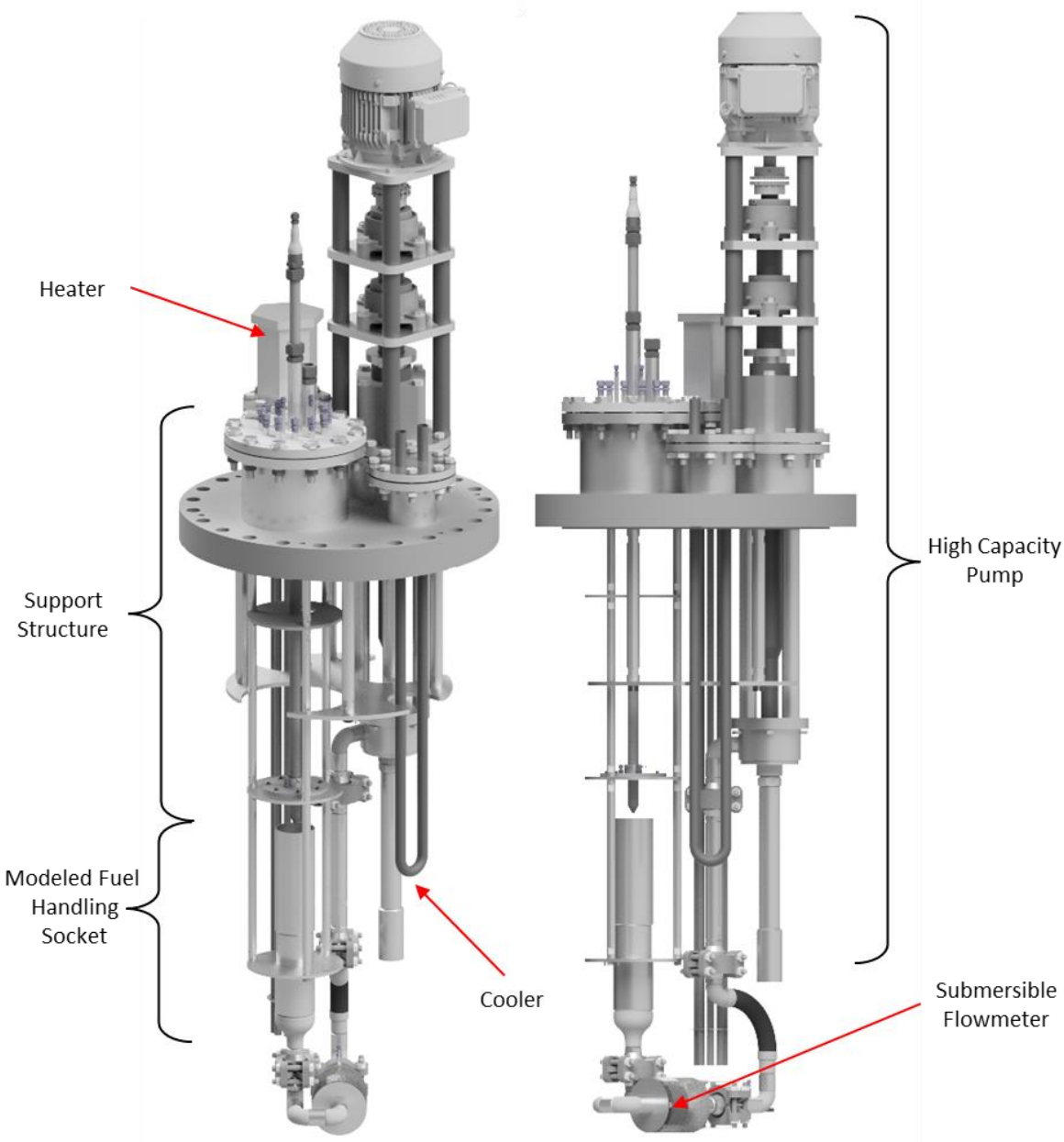

Figure 1 – Two 3D model views of F-STAr with the Full-Scaled Test Section installed.

Initially, F-STAr will be configured to test liquid metal flow sensors, specifically field shift sensors like the Eddy Current Flow Sensors (ECFS) based on the RDT C4-7T standard. To test these sensors, two test sections were designed that attempt to model Sodium Fast Reactor (SFR) outlet conditions. Figure 2 shows models of the "Full-Scaled Test Section" (FSTS) that represents a generic SFR fuel handling socket and a "Pseudo-Scaled Test Section" (PSTS) that represents a generic array of scaled fuel handling sockets.

While F-STAr will be configured to test ECFS's, it can also be outfitted to meet other experimental needs. For example, F-STAr could be setup with a test section that includes a fluidic diode or a component test investigating the performance of hydrodynamic bearings. Other test sections include studies of sodium thermal hydraulics like thermal striping. Overall, F-STAr is a flexible test article designed to accommodate many needs.

This report will provide a status update on the design and construction of F-STAr. Manufacturing of all components has commenced, and several components have already been completed. These components include the pump and test section assembly stand. Other components, such as the heater, have been completed but were rejected due to the vendor not meeting the requirements of the purchase order. Lastly, the submersible flowmeter and main flange components are under construction, and their status will be reviewed in this report. Overall, most of the F-STAr components and parts will be completed by the end of September 2022.

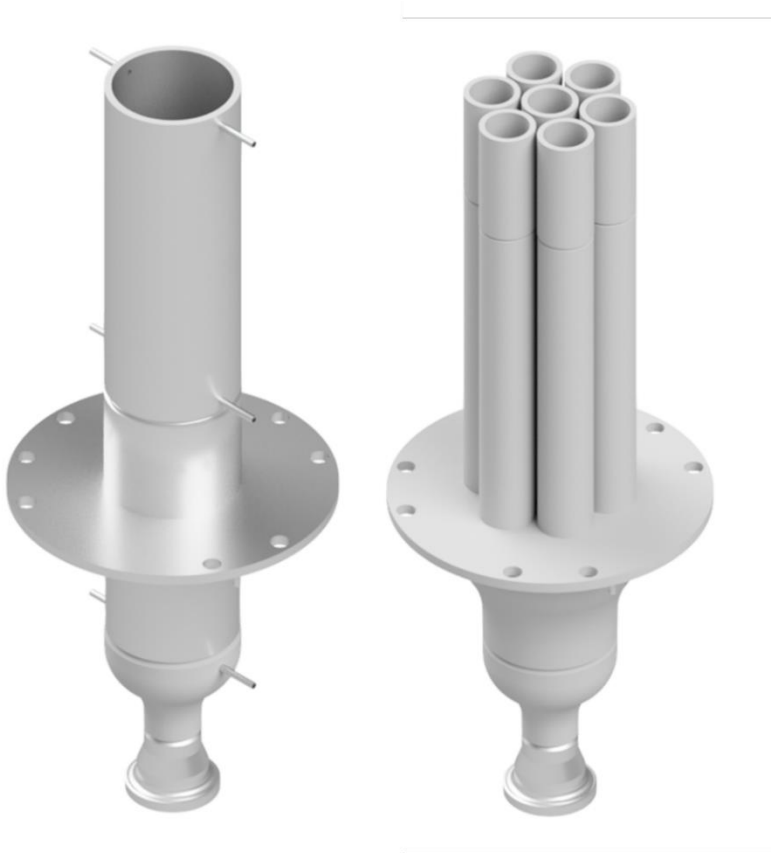

Figure 2 – 3D model view of the Full-Scaled Test Section (left) and Pseudo-Scaled Test Section (right). These test sections have been designed to model the discharge from Sodium Fast Reactor fuel subassemblies.

2 Introduction

Many advanced nuclear power reactor designs are leveraging the unique thermal properties of liquid metals for their primary system coolant. Compared to water, liquid metals have exceptionally good heat transfer properties and high boiling points. Specifically, sodium is unique among liquid metals as its fluid properties at operating temperature are comparable to water. Consequently, several advanced designs, such as the Sodium Fast Reactor (SFR), have selected sodium as the primary coolant.

During reactor operations, flowrate instrumentation is essential for monitoring conditions in and around the core. One class of instrumentation unique to liquid metals are sensors based on Lorentz Force principles. These types of sensors can generate an induced signal in the presence of a magnetic field that is directly proportional to the liquid metal velocity. In some cases, these velocities can be large. For example, SFRs with flowrates of 50,000 GPM or higher can have core fluid velocities as large as 30 ft/s [1] [2] [3] [4] [5] [6] [7]. Additionally, sensor types based on measuring field shifts, like Eddy Current Flow Sensors (ECFS), may also be sensitive to their boundary conditions.

This presents a challenge in the development and testing of field shift type sensors. Matching the high velocities in a SFR subassembly requires large capacity pumps. Additionally, testing in similar boundary conditions requires the sensor to be submersed in a jet exiting a full-sized subassembly. Unfortunately, these facilities are nonexistent, meaning that accurate testing and calibration of these sensors in prototypic conditions cannot be performed.

To address this technology gap, a new METL test article called the Flow Sensor Test Article (F-STAr) was developed. Figure 3 shows a 3D model of F-STAr with some of the main components identified. These components include a high-capacity pump capable of producing a nominal flowrate of 120 GPM; a support structure that can accommodate numerous sensor studies, instrumentation, hydraulic components, and more; and lastly a heating and cooling system to achieve a variety of conditions required by the experimenter. These components are connected in an open loop that uses both the vessel and piping. Figure 4 presents a P&ID diagram showing the general flow path. This open path attempts to mimic the discharge of fluid from a subassembly into a SFR hot pool.

Initially, F-STAr will be configured to test liquid metal flow sensors, specifically ECFSs. During the design of the flow sensor setup, target flowrates and geometric conditions were identified in a literature review of several SFR designs. Table 1 presents the parameters used during the design of F-STAr. Specific reactors that informed the F-STAr design include the ABTR, AFR, ALMR, FASTER, and PRISM as well as others [1] [2] [3] [4] [5] [6] [7]. Since the specifics of each design varied widely, nominal values were chosen to represent a generic reactor.

This report will provide an update on the status of the F-STAr design and construction. Manufacturing of all major components has commenced, and several components have been completed and delivered. Specifically, these components include the pump and test section assembly stand. The heater was also completed and delivered but was rejected due to the vendor not meeting the requirements of the purchase order (PO). Lastly, the submersible flowmeter and main flange components are nearly completed, and their status will be reviewed in this report.

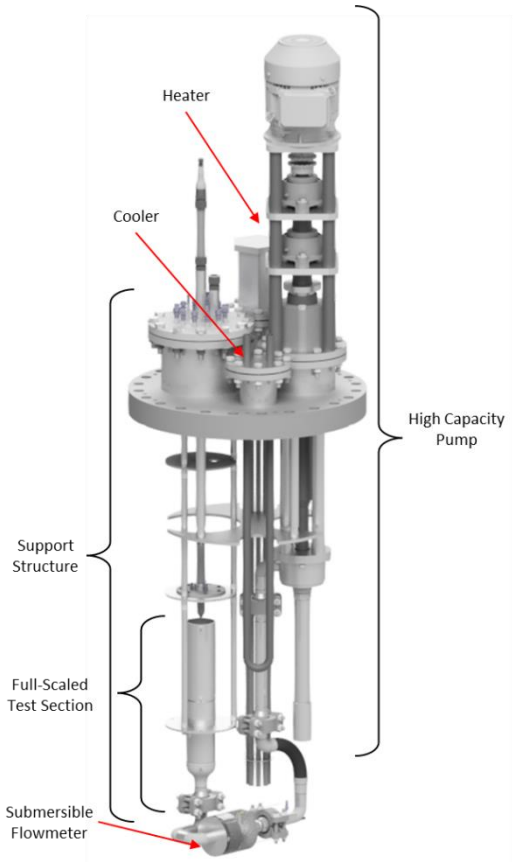

Figure 3 – An isometric view of F-STAr with the main test article components annotated.

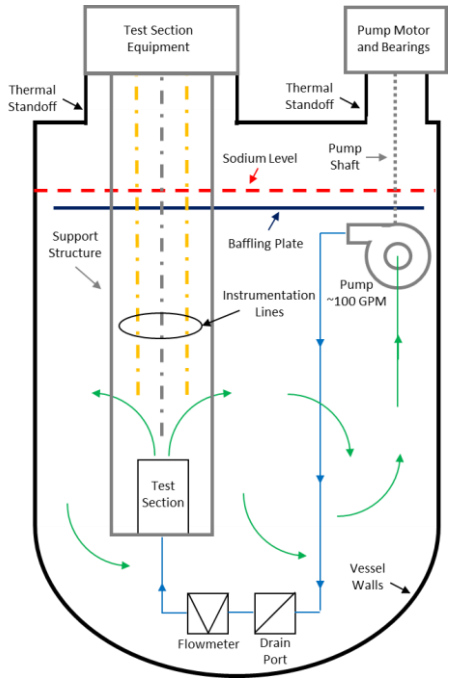

Figure 4 – A simplified P&ID diagram of F-STAr.

Table 1 – Updated F-STAr design parameters for the Full-Scaled and Pseudo-Scaled test sections. These parameters were based on prototypical SFRs. Note that the temperature is limited by components in the flowmeter and the flowrate is limited to the pump performance.

Parameter	Units	Full-Scaled	Pseudo-Scaled
T	*F/C*	930/500	930/500
Assem. Flowrate	*GPM*	120	17
Socket Inner-Diameter	*in*	4	1.5
Socket Length	*in*	12	4
Socket Pitch	*in*	-	2.0
UIS Height	*in*	3	3

3 Design Changes

Since the previous report, a few design changes were made. These changes were a result of additional analysis and needs identified later. However, some changes were a result of meeting the capabilities of the vendor contracted for the construction of components. The vendor specific adjustments were analyzed and were found to have little impact on the performance of F-STAr. In total, these changes are summarized in the sections that follow.

3.1 Test Section Flange

An error occurred during manufacturing of the Test Section Flange. Figure 5 shows a comparison of the as-designed and as-built views. Note that the central holes, designed to align the rabbit tube with the test sections, were machined with a pitch of 2-inches versus 2.1-inches. This error was significant enough that remanufacturing the entire piece would incur a lengthy delay. Therefore, the downstream effects of this error were investigated.

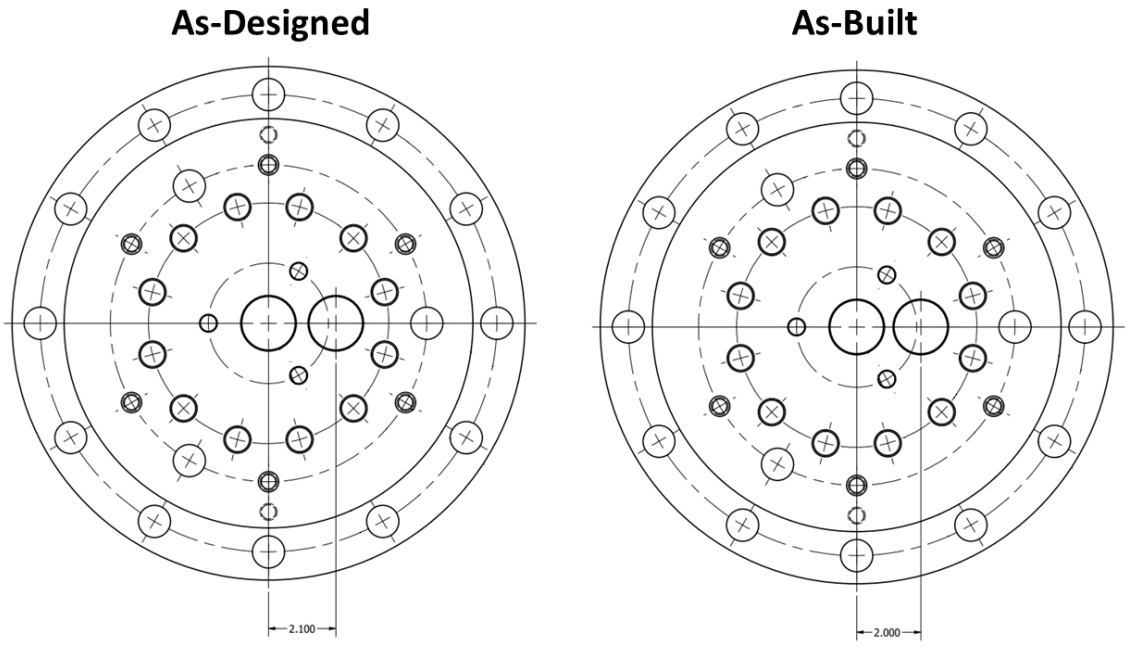

Figure 5 – As-designed configuration of the Test Section Flange compared to the as-built configuration.

Two downstream effects were identified. The first effect was potential interferences during assembly and operation. However, this effect was quickly determined to have no impact on the assembly. The second, more significant effect was on the pseudo-scaling methodology. Therefore, the impacts of the pitch required some additional analysis.

As described in the previous report, the pseudo-scaling methodology began by fixing the desired full-scaled subassembly geometry. Table 2 presents some of these fixed full-scaled parameters. Note that the socket diameter, socket-width ratio, width-pitch ratio, and exit velocity were obtained from average values found in literature review [1] [2] [3] [4] [5] [6] [7]. These parameters were used as inputs to the pseudo-scaling analysis. The results of the initial calculations showed that a flowrate of 730-GPM was required to achieve an 18.7-ft/s velocity from a 4-inch diameter socket. However, reaching this flowrate required a pump that was extremely large and complex. Therefore, a compromise was made for a lower target flowrate of 120-GPM. This target flowrate was estimated as the maximum capacity of the largest pump that could fit in a 28-inch vessel while leaving enough space for a test section. Consequently, the average exit velocity from a 4-inch socket at 120-GPM was calculated as 3-ft/s.

Table 2 – Full-scaled geometric inputs to the pseudo-scaling analysis. Note that the average exit velocity of 18.7-ft/s would require a maximum flowrate of 730-GPM. However, since the pump was designed to produce a maximum flowrate of 120-GPM, the maximum exit velocity is 3-ft/s.

Parameter	Value	Unit
Socket Diameter (D_s)	4	*inches*
Socket-Width Ratio (D_s/D_d)	0.75	-
Width-Pitch Ratio (D_d/p_d)	0.97	-
Width (D_d)	5.3	*inches*
Pitch (p_d)	5.5	*inches*
Average Exit Velocity	18.7	*ft/s*
Average Flowrate (Q_0)	730	*GPM*
Maximum Flowrate (Q_{pump})	120	*GPM*
Maximum Velocity	3	*ft/s*

Next, the parameters in Table 2 were used in the pseudo-scaling analysis to calculate a scaled socket diameter and pitch by matching the exit velocity. Table 3 summarizes the results of this analysis. Since the maximum total flowrate across the array is 120-GPM, achieving an exit velocity of 18.7-ft/s would require a socket diameter of 5/8-inches and a pitch of 0.85-inches. This was found to be too small to accommodate the 1-inch to 1.25-inch diameter ECFS. Therefore, the slower 3-ft/s velocity was matched from the FSTS which resulted in a socket diameter of 1.5-inches and a pitch of 2.1-inches.

Table 3 – Results of pseudo-scaling analysis for an 18.7-ft/s and 3-ft/s socket velocity.

Parameter	Units	18.7-ft/s Exit Velocity	3-ft/s Exit Velocity
Number of Assemblies	-	7	7
Flowrate-per-Assembly	*GPM*	17	17
Scaled Socket Diameter	*inches*	0.62	1.52
Scaled Pitch	*inches*	0.85	2.09

Note in Table 3 that the 2.1-inch pitch is a direct result from the geometric inputs selected in Table 2. Specifically, the perturbations in the pseudo-scaling analysis showed that the socket diameter and associated subassembly width, pitch, and exit velocity significantly impacted the scaled outputs. Figure 6 presents these inputs across several SFRs in categories of experimental, demonstration, and commercial. Note that the horizontal black lines show the values selected for the pseudo-scaling methodology inputs. Figure 6 shows that these inputs vary widely across SFR designs. Consequently, perturbations in these full-scaled inputs can result in the scaled outputs to be above or below the calculated 2.1-inch pitch. Specifically, a 2-inch pitch could be recovered by setting the socket-width ratio to 0.8, resulting in a subassembly width of 5-inches. Overall, the mission of the F-STAr and the design of the pseudo-scaling analysis was to model a "generic" SFR. Therefore, it's inputs may also be non-specific and generic. Consequently, the 2.1-inch value as designed was deemed not critical.

In summary, the as-built configuration of the test section flange was accepted. Drawings of that series were revised, and a new drawing package was sent to the vendor. However, one change that was requested was an adjustment of the rabbit tube clearance opening pitch in the test section baffle plate. Figure 7 shows an elevation view of the baffle plate. This pitch was adjusted from 2.1-inches to 2-inches to ensure enough clearance incase larger instrumentation were to be installed. This will likely not incur significant cost or delay as the features in the baffle plate are simpler and less numerous.

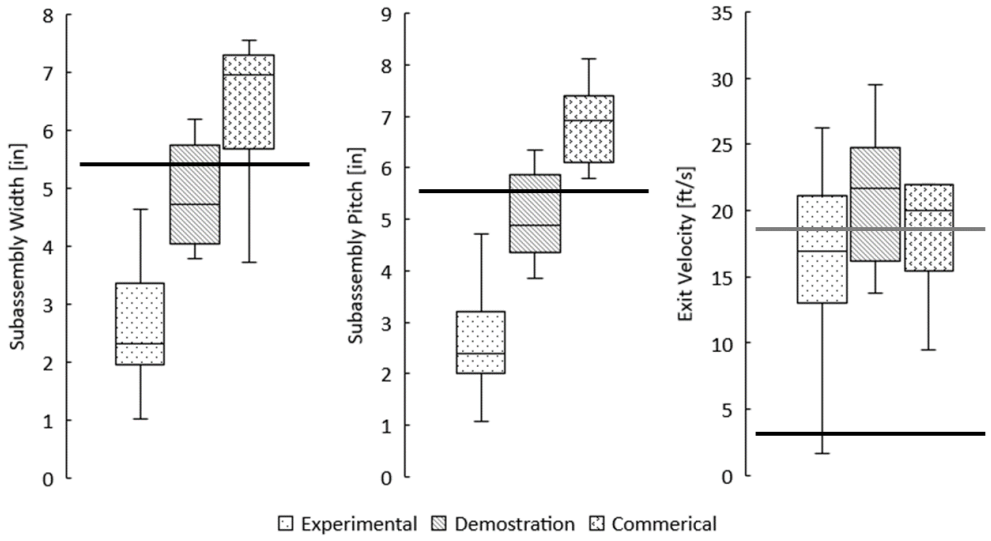

Figure 6 – Fuel subassembly width, pitch, and average exit velocity of several SFR designs in the experimental, demonstration, and commercial categories.

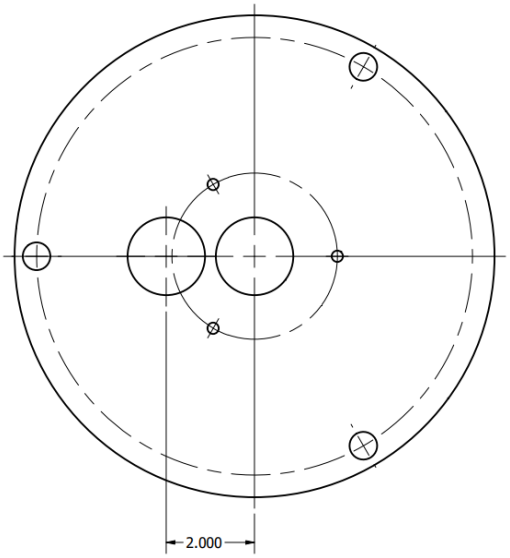

Figure 7 – Updated test section baffle plate with new rabbit tube pitch.

3.2 Pseudo-Scaled Test Section

The Pseudo-Scaled Test Section (PSTS) design was adjusted to account for the 2-inch versus the 2.1-inch pitch. Figure 8 shows an isometric view of the updated design. While much of the original design was left unchanged, the outer diameter of the flow-conditioners was reduced. In the original design, these pieces were to be manufactured from 2-inch diameter round stock. Consequently, the flow-conditioner tubes would contact and potentially trap sodium between them. Therefore, the flow-conditioner outer diameter was adjusted to use 1.875-inch round stock to provide sufficient clearances.

Figure 8 – Updated Pseudo-Scaled Test Section with a new 2-inch pitch and resized flow conditioners.

3.3 Full-Scaled Test Section

Changes in the Full-Scaled Test Section (FSTS) included the addition of three pairs of thermocouple ports. Figure 9 shows an isometric view of the updated model on the left and a sectional view with dimensions on the right. One pair of these thermocouple ports were placed 0.65-inches below the inlet to the flow-conditioner, another pair were placed 0.65-inches above the flow-conditioner, and the final pair were placed 0.5-inches below the socket exit. During the initial testing campaign, these ports will be capped. However, they were included to allow for the possibility of finer flow temperature measurements or pressure measurements.

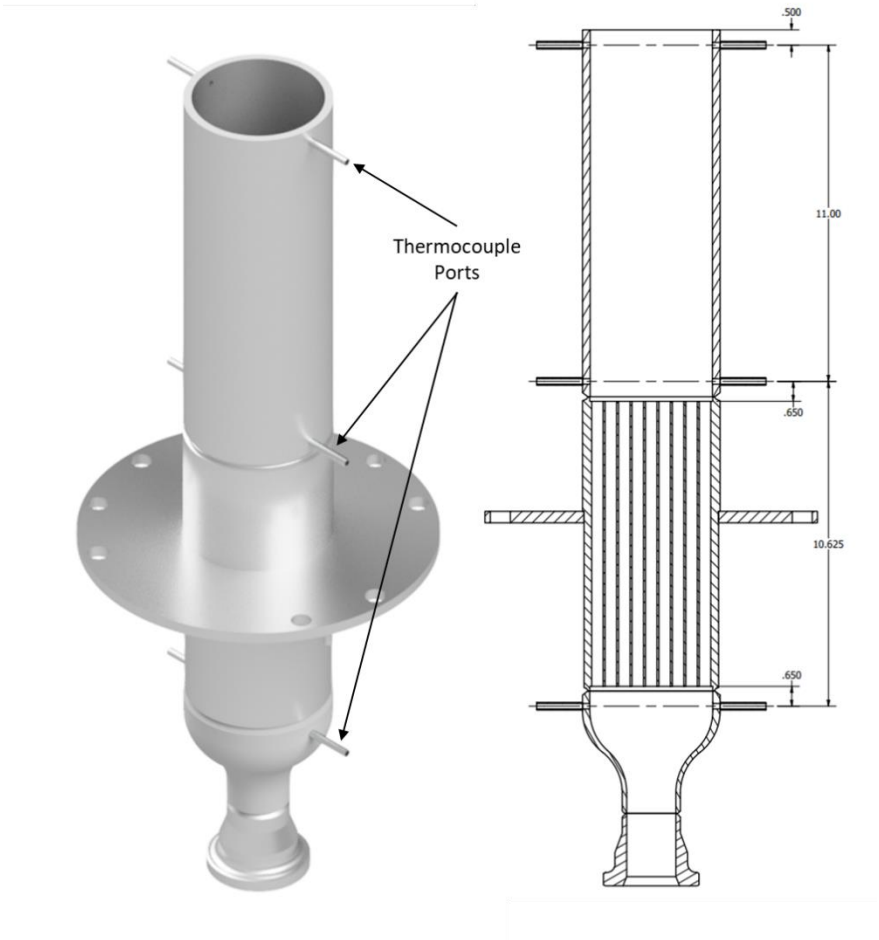

Figure 9 – Updated Full-Scaled Test Section with additional thermocouple ports. Dimension and location of the ports are shown on the right.

3.4 UIS Baffle Plate

The UIS Baffle Plate design was changed to allow more freedom in aligning the rabbit tube. During ECFS calibration it will be important to know the location of the sensor relative to the fuel handling socket. It is assumed that the ECFS calibration is impacted by the socket geometry due to the driving fields extending into it. Therefore, if the sensor were placed closer to one wall of the socket versus the other, the calibration curves may differ. Figure 10 shows the initial test section design. In the initial design, the alignment of the sensor was fixed at two locations; a top support was used to fix the lateral and vertical location and a bottom support was used to fix the lateral support but allow the sensor the move vertically for thermal expansion. It was assumed this method would be sufficient for fixing the sensor in a known location relative to the socket.

However, this design was created with an assumption of near-perfect tolerances. To account for the cumulative effect of as-built tolerances, a stacking analysis was completed. Note that from the test section flange to the test section base plate, seven components are stacked. Figure 11 highlights these seven components and Table 4 specifies the tolerances of each component that were used in the analysis. Assuming the worst case, the stacking analysis showed that the test section flange and FSTS could be off center by about 0.125-inches.

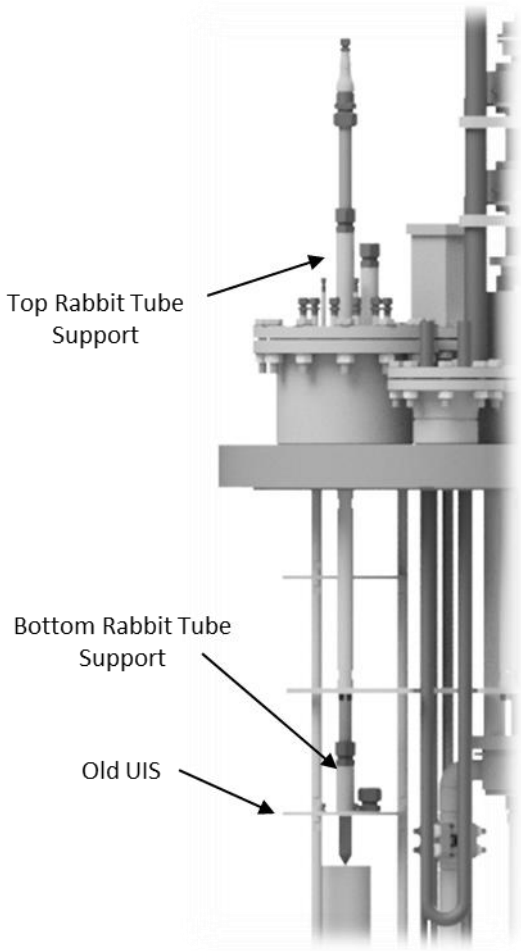

Figure 10 – Elevation view of Test Section support structure with old UIS design. In this design, the UIS fixed the rabbit tube laterally while allowing it to move vertically for thermal expansion.

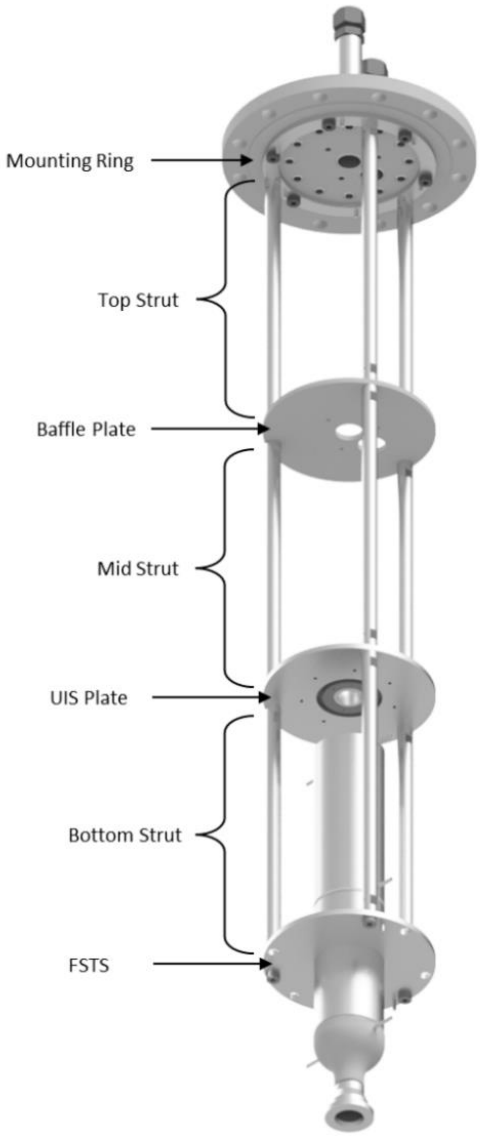

Figure 11 – Isometric view of Support Structure with Full Scaled Test Section installed with labeled components considered in the tolerance stacking analysis.

Table 4 – Table of tolerances used in Test Section stacking analysis.

Component	Parallelism Tolerance	Units
Mounting Ring	0.002	*inches*
Top Strut	0.0005	
Baffle Plate	0.002	
Mid Strut	0.0005	
UIS Plate	0.002	
Bottom Strut	0.0005	

To account for manufacturing tolerances, the UIS plate was redesigned to allow for adjustment of the rabbit tube in the lateral direction. Figure 12 shows two isometric views of the updated UIS plate, one from above and one from below. The new design allows for two types of lateral adjustment. The first is a course adjustment achieved by the seven slotted holes. These allow the top plate to be moved by 0.375-inches in either direction of the slots. The top plate can be rotated to change the direction of the adjustment. The second is a fine adjustment achieved by three set screws. These allow for the rabbit tube to be adjusted in the small areas not covered by the course adjustment.

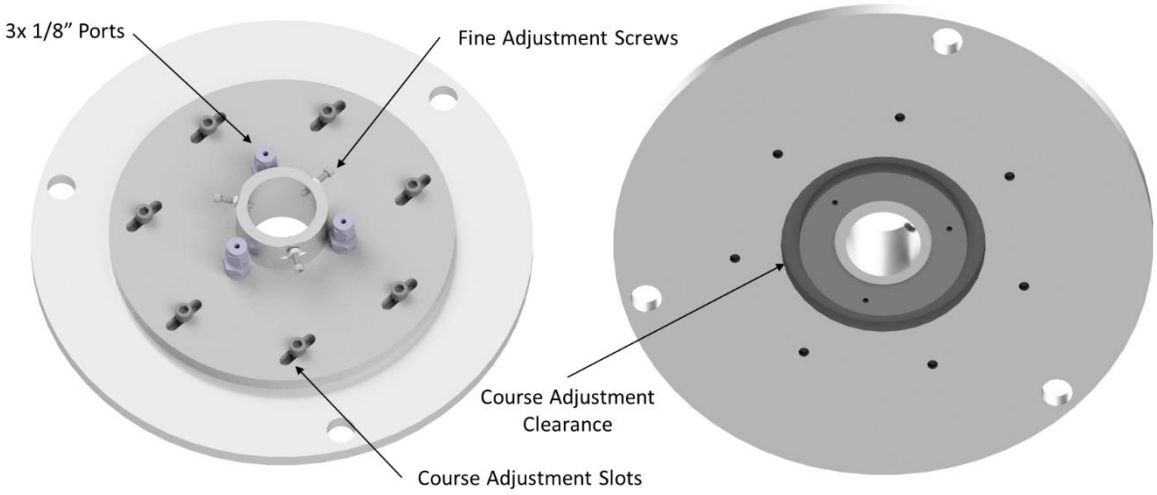

Figure 12 – Updated UIS baffle plate that allows for adjustment of the rabbit tube location about the outlet socket.

3.5 Main Flange

The tolerances on the main flange were adjusted at the request of the manufacturer. Figure 13 shows the as-designed tolerances compared to the as-built tolerances. Specifically, the flatness and parallelness tolerance were doubled from 0.004-inches to 0.01-inches. Additionally, the height tolerance was increased from 0.02-inches to 0.06-inches. These changes will likely have a marginal impact on the overall assembly. However, the vendor was asked to leave enough material on the flange faces so that, in the worst scenario, they could be re-machined.

HeliCoil inserts were added to the bottom of the flange where the baffle plate struts attach. This was done to prevent seizure of the strut threads into the main flange. While it is unlikely that these threads will see any wetting by sodium, they may see vapors at high temperatures. Since the main flange is a significant piece of the assembly, any chance of threads seizing is unacceptable. Therefore, HeliCoils were specified to address this concern.

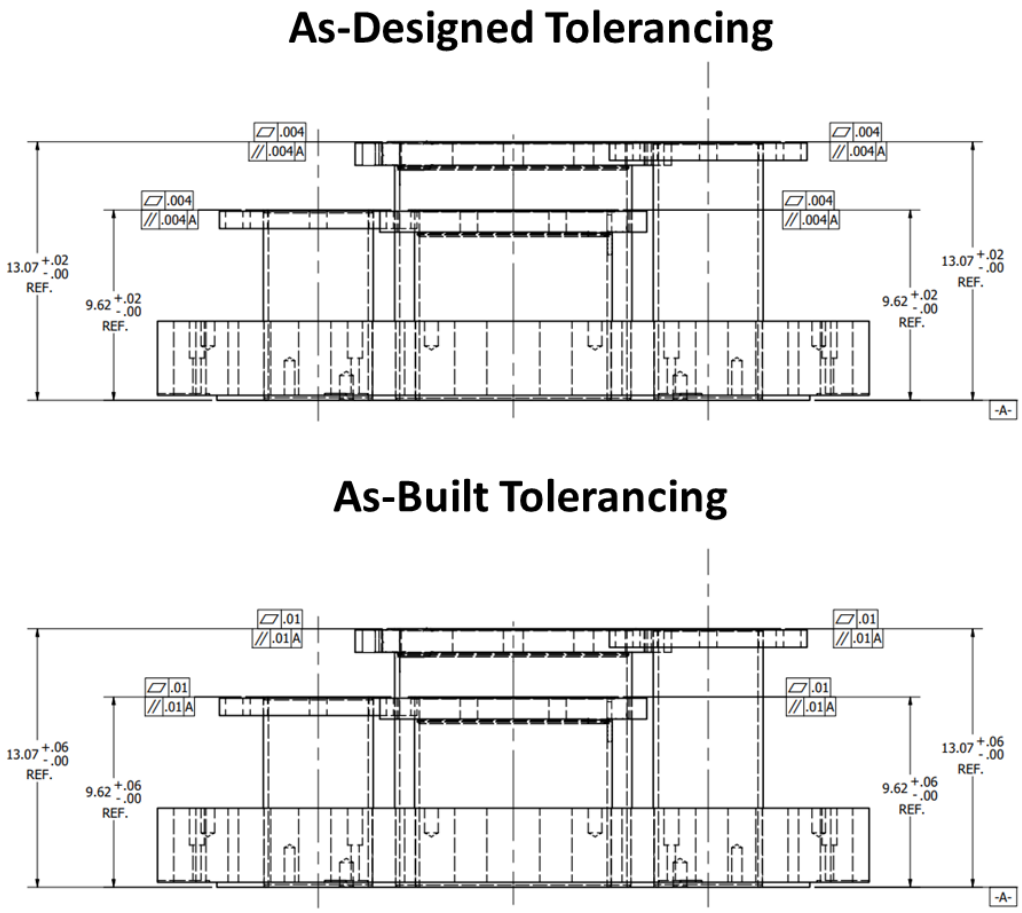

Figure 13 – Dimensions and tolerancing of the Main Flange Weldment. The as-designed tolerancing was found to be too restrictive for the manufacturer. Therefore, the tolerances were increased. This will likely have little impact on the final assembly as none of the sub-flange components need precise alignment at the bottom of the vessel.

3.6 Plumbing

Adjustments were made to the flexible hose located near the pump discharge. Figure 14 shows a comparison of the as-designed and as-built dimensions. During manufacturing, it was difficult to accommodate the exact radius specified in the drawing. Since this piece will not see much movement and only account for a small displacement in thermal expansion, the radius dimension tolerances were opened. After construction, the dimensions were slightly smaller than specified, but this will likely cause few issues. Additionally, the drain tube location was changed. Figure 15 shows the new location of the drain tube being flush with the inner diameter of the elbow. This was changed due to concerns with trapped sodium volumes beneath the drain tube inside the elbow.

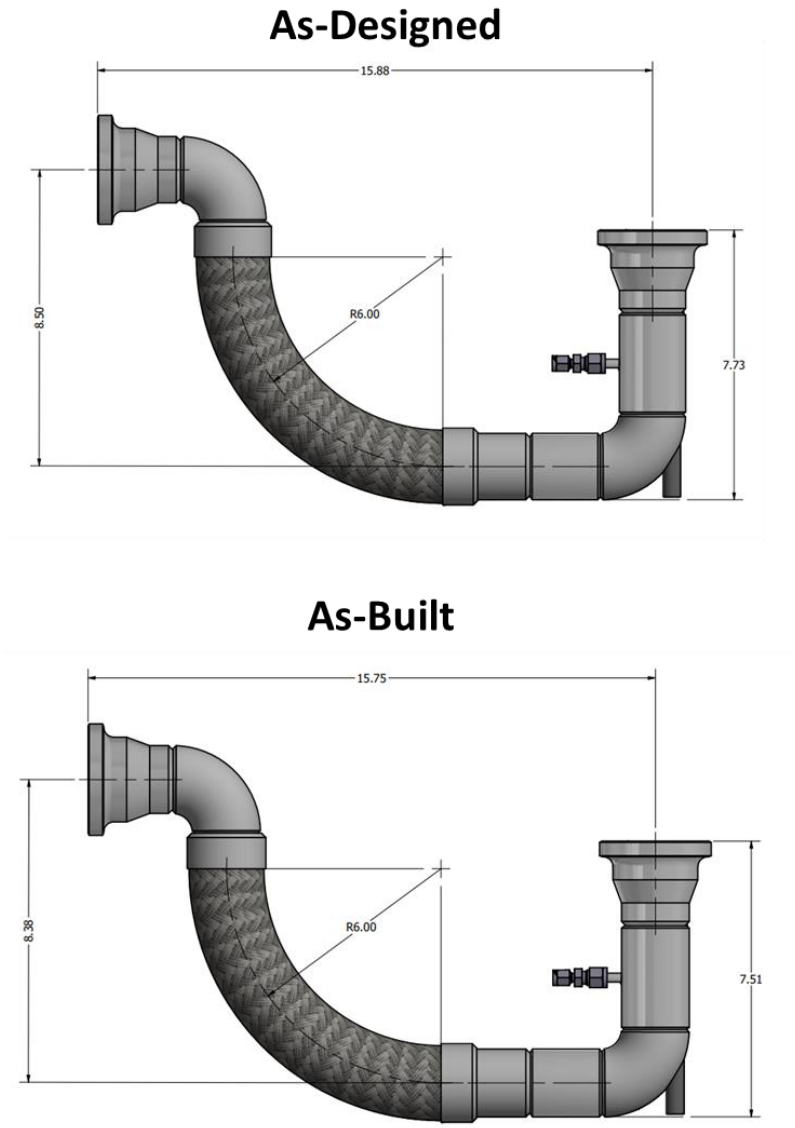

Figure 14 – Dimensions of the flex-hose in the initial design compared to the as-built configuration.

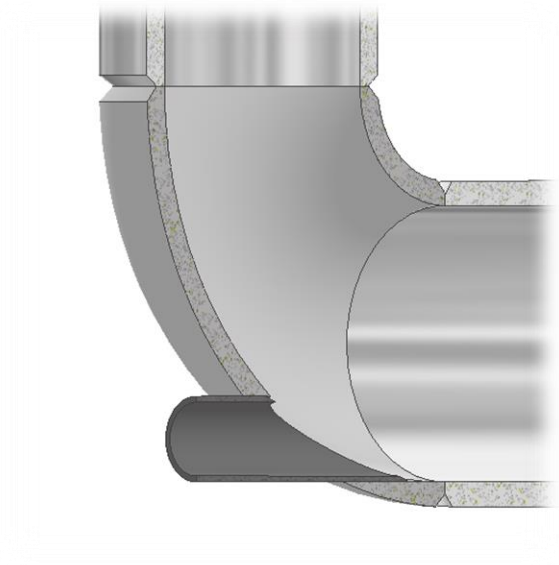

Figure 15 – New drain tube design places tube flush with the elbow.

3.7 Flowmeter

Several adjustments were made to the submersible flowmeter. Figure 16 shows an isometric view of the updated model. Firstly, a 0.25-inch outer diameter snorkel tube was added. This tube will allow control of the environment on the inside of the flowmeter. For example, the internals could be inerted with argon, nitrogen, or helium; or a vacuum could be pulled on the flowmeter. This will be beneficial as the magnet coating can degrade when exposed to oxygen at high temperatures. Secondly, the connections for the signal leads and thermocouples were adjusted to improve the assembly. Lastly, the conduit was lengthened at one end to allow for installation into a calibration setup.

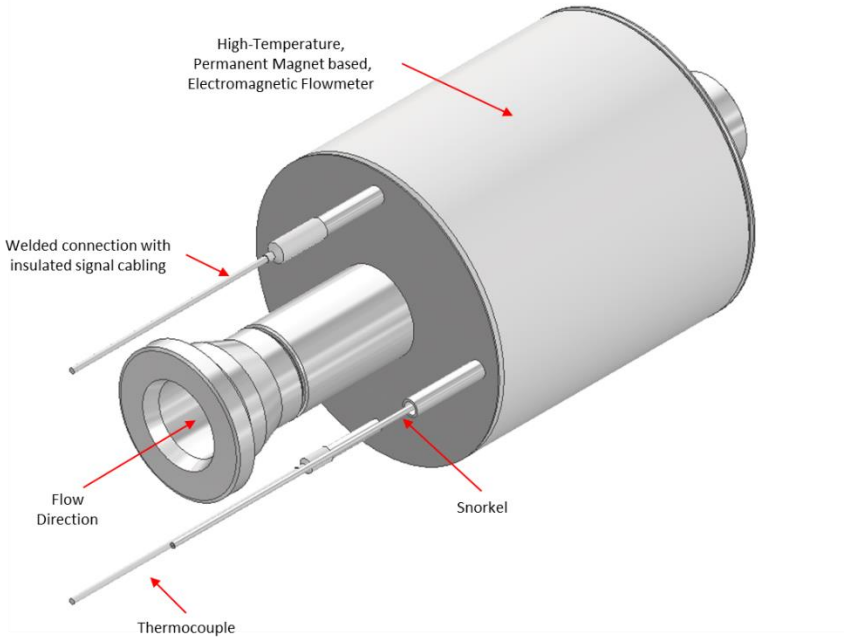

Figure 16 – Updated flowmeter design that includes an 1/8-inch snorkel tube. This tube will be routed through the test section flange and allow the internal flowmeter environment to be controlled during testing.

4 Fabrication Status

Manufacturing of F-STAr was split-up between several vendors and components. Figure 17 summarizes the breakdown of F-STAr components into the pump, heater, flowmeter, test section assembly stand, and finally the balance. At the time of this report, the pump has been constructed, tested, received, and is currently in storage. Additionally, the heater has been completed. However, documentation and testing were not provided, and the heater was rejected. Consequently, it was sent back to the vendor for the required testing.

Two vendors participated in the construction of the flowmeter. A magnet vendor was selected to construct and fixture the magnets while a machine shop was selected to fabricate the balance of the flowmeter. At the time of this report, the magnet construction has been delayed due to material block issues. As for the balance of fabrication, all material was purchased and machined.

The Test-Section Assembly Stand was also completed, received, inspected, and accepted with no exceptions. It is currently in storage with the other received components. Finally, the balance of F-STAr is roughly 80% complete. Some delay was incurred during manufacturing caused by issues with machining some features on the main flange.

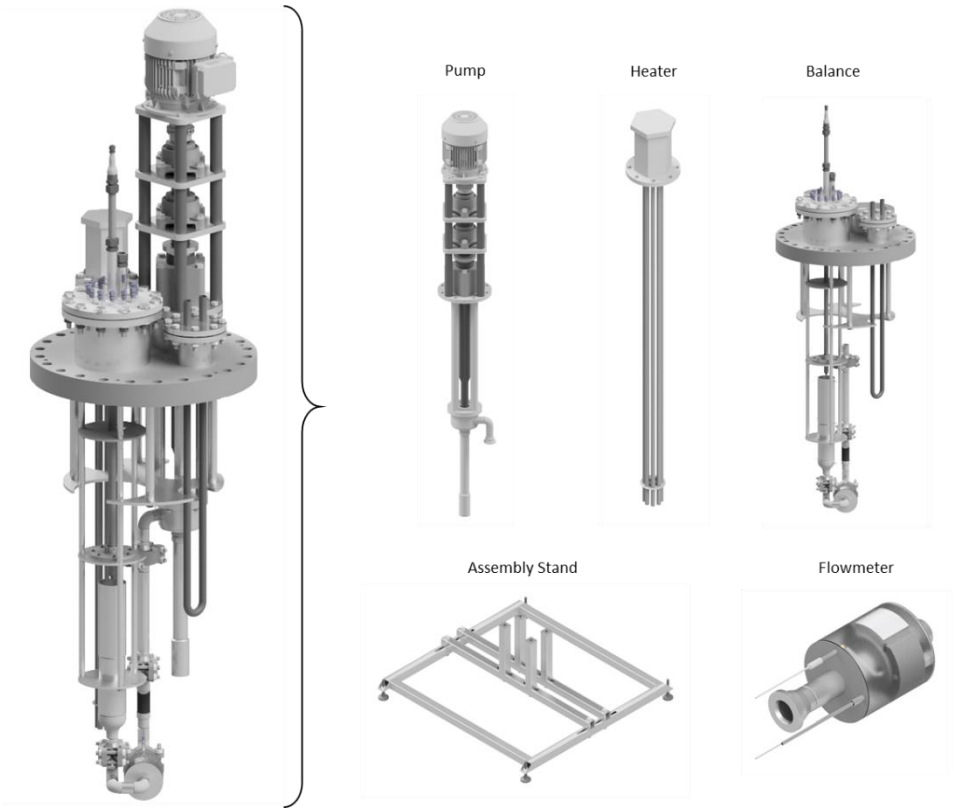

Figure 17 – Breakdown of F-STAr components contracted to unique manufacturers.

4.1 F-STAr Pump

A PO was issued for the construction of the F-STAr pump on 07/19/2021. Construction progressed rapidly and the pump was tested on 12/01/2021. Figure 18 shows the completed pump at the vendor setup for initial testing. Table 5 provides some of the initial validation data obtained in water at the vendor. The maximum flowrate measured was just over 105-GPM at 83% of the maximum rated speed. These data suggest that pump should achieve the maximum specified flowrate of 120-GPM. After testing and validation, the pump was shipped and received on 12/08/2021. Currently, the pump is wrapped and in storage.

Figure 18 – Completed pump setup at vendor for initial validation testing.

Table 5 – Pump data obtained during initial validation testing. The maximum speed tested was 83% with a recorded flowrate of over 105 GPM. These data suggest that at the maximum rated speed, the pump should achieve the maximum specified flowrate of 120 GPM.

Speed [%]	Flowrate	Units
42	60	*GPM*
83	106	*GPM*

4.2 Heater

A PO was issued for the construction of the heater on 08/04/2021. During the unit construction several issues occurred. Firstly, the vendor could not source the originally specified Incoloy-800 tubing for the heating element sheaths. Therefore, the manufacturer suggested using Incoloy-600 as an alternative. This change was investigated and accepted. However, the vendor still had issues sourcing the new alloy. Additionally, the vendor experienced management and labor turnover during construction of the heater. Both issues contributed significantly to delays in construction.

After over ten months, the unit was delivered on 06/15/2022. Figure 19 shows a photo of the crated heater after arrival. Resistance testing was completed on each of the heating elements, lug-to-lug, and lug-ground. Table 6 summarizes the testing results and overall, the elements appeared to be within the desired specifications. However, further inspection revealed that the requested MTRs, hydrostatic test, and dye pen testing documentation were not included. After several inquiries to the vendor, it was discovered that this documentation was never included, and the testing was never completed. Therefore, the unit was rejected and returned to the vendor for the required testing to be completed.

Figure 19 – Crated heater unit after arrivial. The unit passed the resistance testing on the heating elements. However, MTR, dye-pen testing, and hydrostatic testing documentation were not included and were later found to be omitted during construction. Therefore, the unit was rejected and returned to the vendor for the required testing.

Table 6 – Table of resistances measured on each heating element. Note that the resistance between each element's lug to its respective sheath was measured.

Element [#]	Lug-Lug [ohm]	Lug*-Sheath [G-ohm]
1	402	
2	399	
3	403	
4	404	
5	398	>50
6	402	
7	400	
8	400	
9	401	

*Left lug-sheath and right lug-sheath.

4.3 Submersible Flowmeter

In total the submersible flowmeter work was separated between two vendors. One vendor handled the magnet manufacturing while another vendor handled the balance. The magnets used in the flowmeter are custom, high temperature SmCo magnets. Because of their high magnetic field strength, the magnet vendor work scope also included fixturing the magnets to the yoke. Figure 20 shows the final assembly to be provided by the magnet vendor. Note, that the manufacturing of the yoke was not included in the magnet vendor work scope. A PO for the construction and fixturing of the magnets was sent to the vendor on 02/22/2022. The yoke was completed first and then shipped to the vendor on 05/17/2022. At the time of this report, the magnet construction has been delayed due to material block issues. Consequently, the magnet blocks needed to be remanufactured. Currently, the expected delivery date of the magnet assembly is 09/09/2022.

A PO for the balance of the flowmeter construction was sent to a different vendor on 03/22/2022. At the time of this report, all material has been acquired and as much fabrication as possible has been completed. Progress will continue once the magnet assembly is received from the vendor. The completion date of the flowmeter is expected to be roughly 2-3 weeks after receiving the magnet assembly.

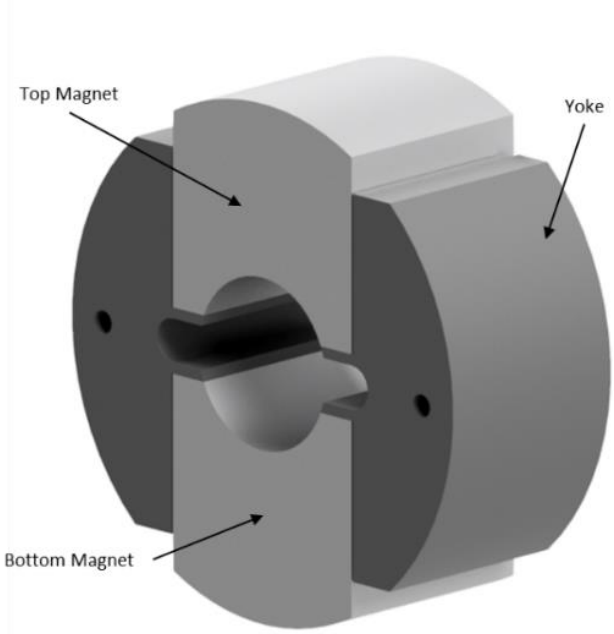

Figure 20 – Model of the final flowmeter magnet assembly. The magnet vendor scope included manufacturing the magnets and fixturing them to the yoke. However, it did not include manufacturing the yoke itself.

4.4 Test-Section Assembly Stand

A PO was issued for the construction of the test-section assembly stand on 01/26/2022. The stand was received on 03/08/2022. Figure 21 shows the completed assembly in storage. Dimensional checks were made and found to be within specifications and the stand was accepted. Future work will include giving the stand a coat of paint to protect the steel.

Figure 21 – Completed test section assembly stand in storage.

4.5 Balance of F-STAr Components

A PO was issued for the balance of F-STAr components on 03/21/2022. At time of this report, approximately 80% of the work has been completed. Some delay was incurred sourcing a subcontractor to complete cutting the large openings in the main 28-inch flange. The new estimated delivery date of the balance of components is expected in the 3rd week of September.

Below are some photos of the fabrication progress taken during vendor visits. Figure 22 shows the bottom of the Test Section Flange without the fittings welded. Figure 23 shows the alignment piece of the UIS Baffle Plate in the center with the Test Section Support Ring surrounding it. Figure 24 shows the Test Section Support Struts. Figure 25 shows each thermal stand-off for the Main Flange. Finally, Figure 26 and Figure 27 show the Full-Scaled Test Section and flow-conditioner respectively.

Figure 22 – Bottom view of the Test Section Flange. Note that this view is prior to the fittings being welded.

Figure 23 – Rabbit Tube alignment (center) and Test Section Support Ring (outer).

Figure 24 – Test Section Support Struts.

Figure 25 – View of the four main flange thermal stand-offs. On the left is the test section, in the center-back is the pump, in the center front is the cooler, and on the right is the heater.

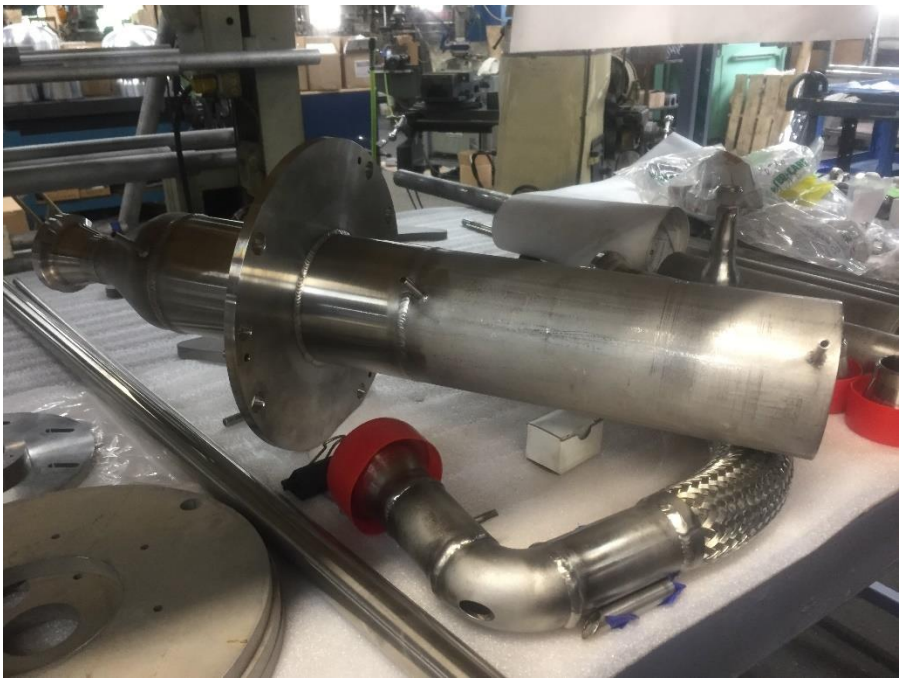

Figure 26 – Photo of the full-scaled test section.

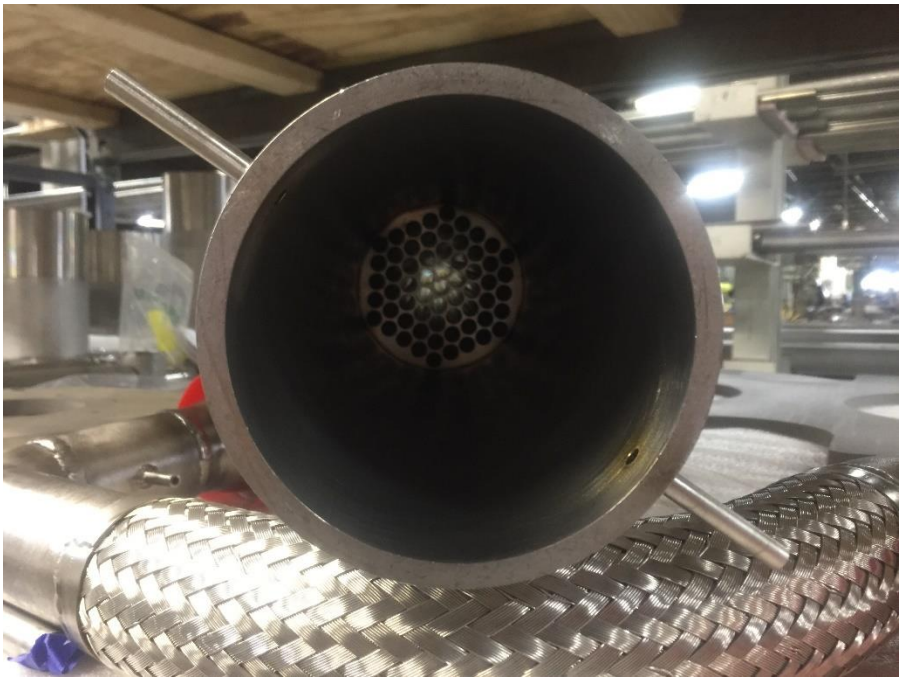

Figure 27 – Inside view of full-scaled test section showing the flow conditioner.

5 Conclusions and Path Forward

Manufacturing of F-STAr components has commenced, and several components have already been delivered. Specifically, the pump was completed ahead of schedule and initial testing demonstrated that it would meet the expected performance requirements. Additionally, the test section assembly stand was completed and is currently in storage. Furthermore, the heater was completed by the vendor, but was missing the required testing. Consequently, the unit was rejected and sent back to the vendor to complete the testing. Lastly, the balance of F-STAr's components are nearly complete and are expected to be received in the 3rd week of September. As for the flowmeter, the magnet assembly is estimated to be shipped on 09/09/2021. Once received, the assembly will be inspected to verify it meets the PO requirements. After the assembly passes inspection, it will be shipped to the vendor and the flowmeter will be finished in the last week of September or first week of October.

The next steps in the F-STAr project will be implementing a Validation and Installation Plan (V&IP). This will include inspecting the received components to ensure they meet the required specifications, as well as dry testing of the pump to verify proper operation. Also included in the V&IP will be extensive water testing to quantify the pump performance and hydraulic characteristics of F-STAr. This testing will also verify the performance of the test sections, instrumentation, and baffle plates. The final steps in the V&IP include installing F-STAr into METL and completing hot-dry testing to verify performance.

For the flowmeter, a few more steps will be included in the V&IP. First, after fabrication, the flowmeter assembly will be installed into a different sodium loop. While installed, the flowmeter will be tested to verify a signal is produced and is in the expected range. Additionally, this testing will allow the sodium to "wet" the conduit walls. Lastly, the flowmeter will be calibrated in sodium over 1-GPM to 20-GPM and 200-^{o}C and 400-^{o}C. These additional tests will fully validate the functionality of the flowmeter.

In summary, this report reviewed the status of the design and fabrication of F-STAr. Since the previous report, a few design adjustments were made in response to analysis and needs identified later. In some cases, these changes were a result of meeting the capabilities of the vendor. The vendor specific adjustments were analyzed and were found to have little impact on the performance of F-STAr. Fabrication has commenced and many components are already finished and delivered, or nearly finished. Some issues have occurred with labor and material issues at vendors, specifically the heater, which have impacted certain aspects of the F-STAr project. Overall, though, the majority of F-STAr components are on track to being completed by the end of September.

6 Acknowledgements

The authors would like to acknowledge METL team member Daniel Andujar for all the hard work and dedication to constructing, maintaining, and operating the facility. This work is funded by the U.S. Department of Energy Office of Nuclear Energy's Advanced Reactor Technologies program. A special acknowledgement of thanks goes to Mr. Brian Robinson, Fast Reactor Program Manager for the DOE-NE ART program, Dr. Bo Feng, the National Technical Director for Fast Reactors for the DOE-NE ART program, and to Dr. Robert Hill, GIF Technical Director for their consistent support of the Mechanisms Engineering Test Loop and its associated experiments, including F-STAr.

7 References

[1] M. El-Wakil, Nuclear Energy Conversion, Scranton, Pennsylvania: Intext Education Publishers, 1971, p. 330.

[2] Argonne National Laboratory, "Advanced Burner Reactor 1000 MWth Reference Concept," Lemont, 2007, ANL-AFCI-202.

[3] Argonne National Laboratory, "Advanced Fast Reactor - 100 (AFR-100) Report for the Technical Review Panel," Lemont, 2014, ANL-ARC-288.

[4] GE Nuclear Energy, "ALMR Summary Plant Design Description," San Jose, 1993.

[5] Argonne National Laboratory, "FASTER Test Reactor Preconceptual Design Report," Lemont, 2016, ANL-ART-86.

[6] General Electric, "PRISM Preliminary Safety Information Document," San Jose, 1987.

[7] IAEA, "Fast Reactor Database 2006 Update," IAEA, Vienna, 2006.

Nuclear Science and Engineering Division
Argonne National Laboratory
9700 South Cass Avenue
Lemont, IL 60439

www.anl.gov

Argonne National Laboratory is a U.S. Department of Energy laboratory managed by UChicago Argonne, LLC